The use of fire at Zhoukoudian: evidence from magnetic susceptibility and color measurements

**Yan Zhang · Zhengtang Guo · Chenglong Deng · Shuangquan Zhang ·
Haibin Wu · Chunxia Zhang · Junyi Ge · Deai Zhao · Qin Li · Yang Song ·
Rixiang Zhu**

Abstract In order to provide direct evidence for the use of fire by humans at Locality 1, Zhoukoudian, we examine the burnt and unburnt sediments of newly excavated area in Layer 4 by detailed measurements of magnetic susceptibility, color, and diffuse reflectance spectrum. Results show that the magnetic susceptibility and redness of the burnt sediments are remarkably higher than those of other areas on the same level: up to ~ 22 times for magnetic susceptibility and ~ 3 times for redness of those of the adjacent unburnt sediments. Fine-grained (superparamagnetic/stable single-domain) magnetite and hematite grains make dominant contributions to the distinctly high values of magnetic susceptibility and redness in the burnt sediments. Diffuse reflectance spectroscopy results show that the burnt sediments contain more hematite than those of other areas and localities 2 and 3. High-temperature magnetic susceptibility measurements demonstrate that the burnt sediments have been heated above 700 °C. Those changes in low-frequency magnetic susceptibility and redness are impossibly resulted from natural fires, thus most likely signaling the human activities of controlled use of fire. However, further work is needed to confirm whether or not these heat-affected sediments were produced in situ.

Keywords Zhoukoudian · Use of fire · Magnetic susceptibility · Redness · Rock magnetism

Y. Zhang · Z. Guo (✉) · H. Wu · C. Zhang · Q. Li · Y. Song
Key Laboratory of Cenozoic Geology and Environment, Institute
of Geology and Geophysics, Chinese Academy of Sciences,
Beijing 100029, China
e-mail: ztguo@mail.iggcas.ac.cn

Y. Zhang · Q. Li · Y. Song
University of Chinese Academy of Sciences, Beijing 100049,
China

C. Deng · R. Zhu
State Key Laboratory of Lithospheric Evolution, Institute of
Geology and Geophysics, Chinese Academy of Sciences,
Beijing 100029, China

S. Zhang · J. Ge
Key Laboratory of Vertebrate Evolution and Human Origins of
Chinese Academy of Sciences, Institute of Vertebrate
Paleoanthropology, Chinese Academy of Sciences,
Beijing 100044, China

D. Zhao
Faculty of Earth Sciences, China University of Geosciences,
Wuhan 430074, China

1 Introduction

The use of fire was one of the most important skills of hominins, which has been reported to go back at least 0.5 Ma, possibly more than 1.0 Ma [1–4]. Locality 1 of Zhoukoudian is one of the earliest sites, in which solid evidence for the use of fire was preserved [5–7]. Excavation of Locality 1 in 1920–1930s yielded the "apparently charred or partly calcined animal bones," "antler samples," and "black layers" [5]. Based on chemical analysis, those materials were suggested to be the "evidences of the use of fire by *Sinanthropus*" [5]. Other materials were also recovered during later excavation, e.g., burnt bones, burnt stones, and charcoal of Chinese redbud [8]. Guo et al. [9, 10] made fission track dating, and found that the sphenes in the ash samples of Layer 4 and Layer 10 were heated above the annealing temperature, further suggesting the presence of burning. Dating results of fission track, electron spin resonance, and paleomagnetism show that the age of Layer 10 is about 0.5 Ma B.P. [1, 9, 11–13]. The latest results of

1014

Chin. Sci. Bull. (2014) 59(10):1013–1020

cosmogenic $^{26}Al/^{10}Be$ burial dating of quartz sediments show that the age of Layers 7–10 could be over 0.70 Ma B.P. [2]. Abundant fire remains preserved in Locality 1 brought the history of human controlled use of fire much earlier at that time.

Recently, the existence of in situ burning in Locality 1 was challenged. Weiner et al.'s [14, 15] reexamination of the evidence in Layer 10 and Layer 4 indicated "the absence of ash or ash remnants (siliceous aggregates) and of in situ hearth features", thus they concluded that "there is no direct evidence for in situ burning", and "most of the fine-grained sediments in the site were water laid". However, Wu [16] and other researchers [17] argued that Weiner et al. [14] only did sampling at western section of Locality 1 and "do not fully address the wealth of data collected at the entire site since the 1930s", thus their conclusions are not convincing.

Fire causes the magnetic enhancement in soils and other sediments [18, 19], which can be attributed to the generation of ferromagnetic mineral phases like magnetite or maghemite during heating [20]. Magnetic analysis has been widely applied for studies of archaeological sites [20–24]. Results of experimental fires also show that magnetic methods can be used to effectively identify the presence of heated area, especially in early sites, where the original features of use of fire are not preserved well [25–28].

Burning also changes color of the sediments. At temperatures between 250 and 400 °C, hematite is produced by dehydration of goethite [29], which is widespread in different kinds of sediments. As a pigment mineral, the increased content of hematite causes the reddish color of the sediments. Early researches of the archaeological sites show that heating produced hematite grains are responsible for the rubification [28, 30]. Therefore, color measurements provide useful information of magnetic minerals.

During the new excavation of Locality 1 started from the year 2009 [31], a series of possible remnants of the use of fire were discovered in Layer 4 [32] of the western section. To reveal the distribution of burnt and unburnt sediments and probe into the nature of the magnetically enhanced sediments, these remnants and sediments on the same level were sampled and examined by magnetic, color, and diffuse reflectance spectrum (DRS) measurements.

2 Materials and methods

The remnants of the use of fire come from the sedimentary layer ∼1 m below the top of Layer 4 at the western section. The excavation area covers ∼30 m^2. The sediments of this level are mainly silts, which are partly cemented with calcite. Large angular breccias of limestone distribute on the excavation surface, which are likely to be the

éboulis [33]. The burnt areas distribute at the north and south ends of the excavation area. In the excavation pit N119E71 at the north, black, reddish-brown, and brownish-
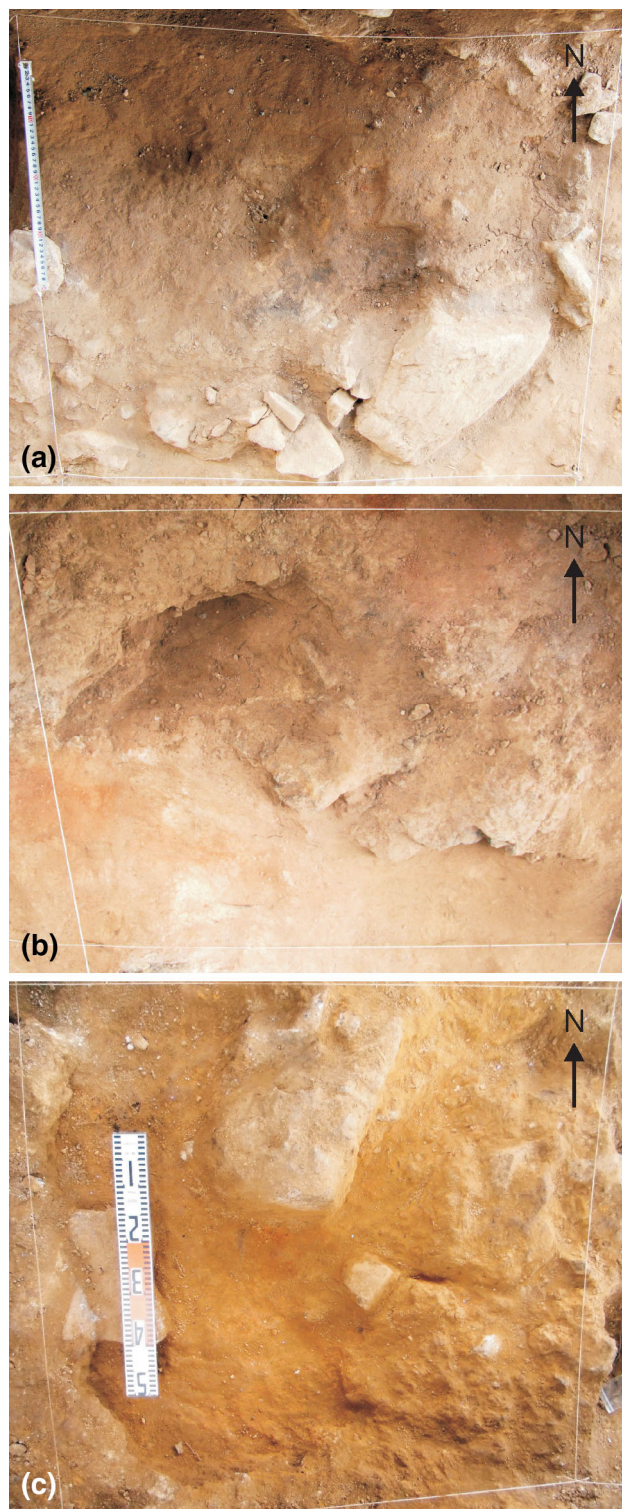

Fig. 1 Photos showing the burnt sediments in areas of H1 (**a**), H2 (**b**), and H3 (**c**). *White lines* indicate borders of the excavation pits (1 m × 1 m)

yellow silty sediments are spotted or banded, and circled by gravels with diameters from ∼2 to 27 cm. This area is named H1 in this study (Fig. 1a). At northwest of H1 and the border of excavation pits N120E69 and N120E70, the sediments are pinkish- or light reddish-brown. This area is named H2 (Fig. 1b). At the south end of the excavation area, the sediments of excavation pit N114E69 and part of N115E69 are orange or orangey-brown, which are distinctly different from yellowish-brown sediments in the adjacent areas (Fig. 1c). This area is named H3 in this study. No distinct horizontal bedding was observed in the field.

In order to detail the sedimentary features of the excavation pits and delineate the range of the burnt area, each pit was gridded for sampling. We collected 36 samples in each pit of the burnt areas, and 9–24 samples in each pit of unburnt areas. Samples were named according to the sampling location. For example, sample ID "N119E71 C3" represents the sample collected at Row C (6 rows were divided equally and assigned A–F, respectively, from south to north of the pit) and Column 3 (six columns were numbered 1–6, respectively, from west to east) of the pit N119E71. Six natural samples were collected as control, including four topsoil samples on the Longgushan Hill, and two samples of red-hue sediments from Localities 2 and 3, respectively [34, 35].

A total of 405 samples were air-dried. Measurements of magnetic susceptibility and color were made on the samples. Magnetic susceptibility (χ) was measured with an Agico MFK1-FA Kappabridge magnetic susceptibility meter at frequencies of 976 Hz (χ_{LF}) and 15,616 Hz (χ_{HF}). The analytical precision is 0.1 %. Two measures of frequency-dependent magnetic susceptibility (χ_{FD}, defined as $\chi_{LF} - \chi_{HF}$, and χ_{FD} %, defined as ($\chi_{LF} - \chi_{HF}$)/$\chi_{LF} \times 100$ %) were calculated from these measurements. Redness was measured by a KONICA MINOLTA CM-700d spectrophotometer. The standard deviation of chromaticity value is within ΔE^{*}_{ab} 0.04.

Following the magnetic susceptibility and redness measurements, typical samples were selected for DRS and high-temperature magnetic susceptibility (χ-T curves) measurements. Firstly, eight samples from the excavation pits and two from Localities 2 and 3 were selected for DRS measurements using a Varian Cary 5000 spectrophotometer equipped with a BaSO$_4$-coated integrating sphere and using BaSO$_4$ as the white standard [36]. Analytical precision of the instrument is 0.5 %. Semi-quantification of goethite and hematite was processed according to the method of Torrent and Barrón [36]. Then, two samples, one from the burnt area and the other from the unburned area were selected for χ-T measurements using an Agico KLY-3 Kappabridge with a CS-3 high-temperature furnace in an
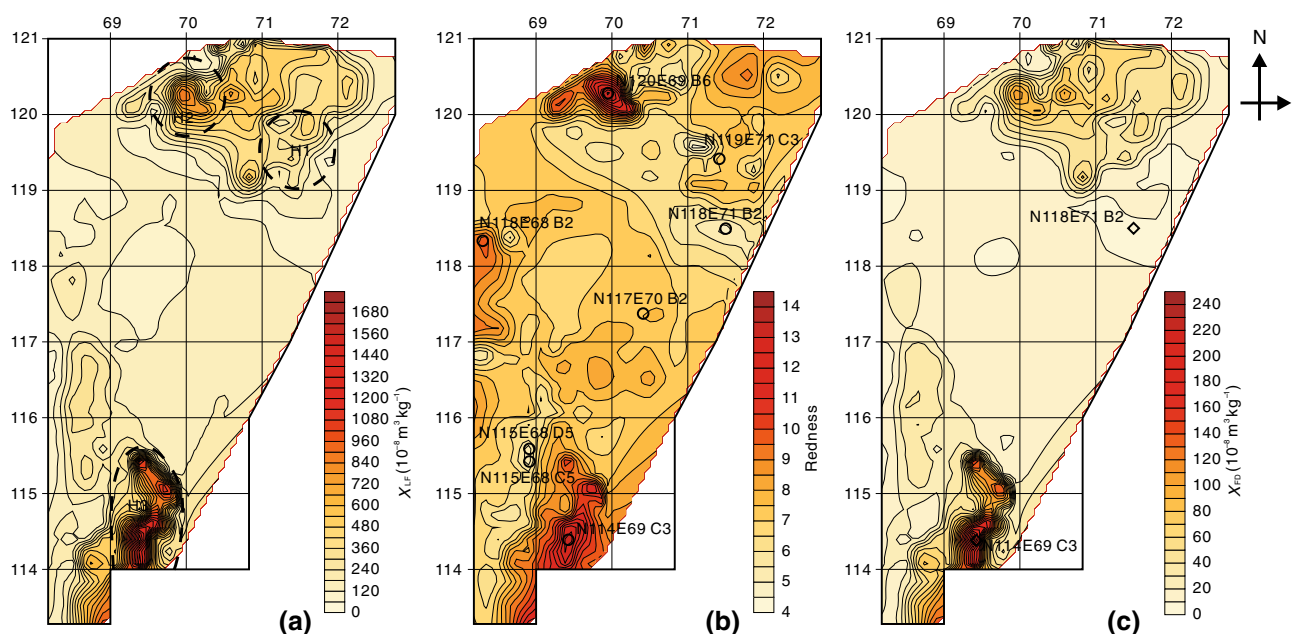
Fig. 2 Contour maps for χ_{LF} (**a**), redness, (**b**) and χ_{FD} (**c**) measurements. The *thick black frame* of each figure represents the range of excavation area. The *thin-line grids* show the excavation pits. The *numbers* outside the frames set the excavation coordinate, according to which the pits were named. The *thick dashed lines* in **a** show the burnt areas. *Black circles* in **b** show the locations of DRS samples (N119E71 C3, N114E69 C3, and N120E69 B6 from the burnt area; and N115E68 C5, N115E68D5, N117E70 B2, N118E68 B2, and N118E71 B2 from the unburnt area). *Diamonds* in **c** show locations of the χ-T samples

1016

Chin. Sci. Bull. (2014) 59(10):1013–1020

argon atmosphere. Each sample was separated into two parts. One was continuously exposed through temperature cycle from room temperature to 700 °C and back to the room temperature. The other was subject to a partial heating/cooling method [37, 38] with the highest temperatures from 100 to 700 °C at an interval of 100 °C.

3 Results

Contour maps for χ_{LF}, redness, and χ_{FD} are shown in Fig. 2. χ_{LF} ranges from 36×10^{-8} to $1,773 \times 10^{-8}$ m^3 kg^{-1}. As shown in Fig. 2a, high values of χ_{LF} mainly occur at the north and south ends of the excavation area. In other areas, χ_{LF} values are relatively lower and show smaller deviations. At the south end, distribution of high χ_{LF} values is consistent with the range of H3, which was delineated during the fieldwork. The highest χ_{LF} value of the whole excavation area is found in the excavation pit N114E69, which is 22 times of that of the adjacent areas. At the north end, the distribution area of high χ_{LF} values is up to 4 m^2, larger than that of the south end; and the values of χ_{LF} are lower than south end. The highest χ_{LF} value is 961×10^{-8} m^3 kg^{-1} in H2, which is 20 times of that of the adjacent areas. The highest χ_{LF} value in H1 is only 514×10^{-8} m^3 kg^{-1}. As a comparison, χ_{LF} values of topsoil samples from the vicinity of Locality 1 are all lower than 180×10^{-8} m^3 kg^{-1}.

Figure 2b shows the contour map of redness, which ranges from 4.6 to 14.3. At the north end, the high values mainly occur in H2, consistent with the field observation. The highest value of 14.3 is at the same place with the highest χ_{LF} value of the north end. H1 shows relatively low redness values, with the highest value 8.1. At the south end, distribution of high redness values is very similar to that of χ_{LF}. The highest value of this area is 13.8, which is at the same place of the highest χ_{LF} value of the whole excavation area. Another high redness region is at the west, of the excavation pits N118E68 and N117E68. The highest value is 9.9, lower than those in H1 and H3. And χ_{LF} values of this area are low (Fig. 2a). Besides, samples of Localities 2 and 3 have quite high redness values (11.3 and 10.6, respectively), but have low χ_{LF} values (120×10^{-8} and 153×10^{-8} m^3 kg^{-1}, respectively).

Frequency-dependent magnetic susceptibility is widely used for detection of magnetic grains ranging across the superparamagnetic (SP) to single-domain (SD) grain size boundary [39]. As shown in Fig. 2c, the distribution of high χ_{FD} values is very similar to that of χ_{LF}. The two parameters are linearly correlated (Fig. 3a). The average and maximum values of χ_{FD} % are 11 % and 15 %, respectively, which suggests that there are considerable quantities of ferrimagnetic grains ranging across the SP to SD grain size boundary, especially in the burnt area with high values of χ_{LF} and redness.
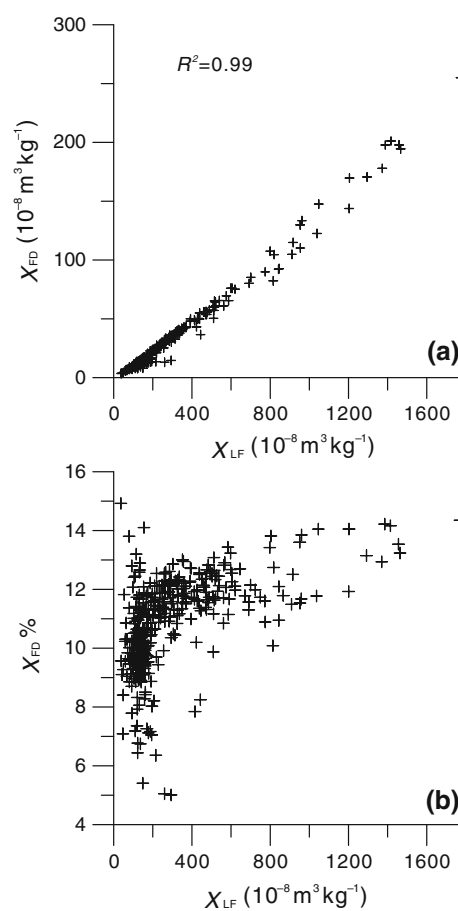
Fig. 3 Relationships between χ_{LF} and χ_{FD} (**a**), χ_{LF} % and χ_{FD} % (**b**)

Figure 4 shows the χ-T curves of sample N114E69 C3 from the burnt area H3 and sample N118E71 B2 from the unburnt area. χ-T curves of the two samples are characterized by a major decrease in susceptibility at ~580 °C (Fig. 4a, i), marking the Curie point of nearly stoichiometric magnetite. In addition, χ-T curve of sample N114E69 C3 from the burnt area is nearly reversible (Fig. 4a). However, χ-T curve of sample N118E71 B2 from the unburnt area is clearly irreversible (Fig. 4i) with the cooling curve above the heating curve. These behaviors suggest that almost no neo-formation of ferrimagnetic minerals during thermal treatment of the sample from the burnt area (N114E69 C3), because the iron-containing silicates/clays in that sample, which are required for generation of strong magnetic minerals, may have been depleted due to the use of fire by hominins [40]. As for sample N118E71 B2 from the unburnt area, large quantity of strong magnetic minerals was generated during thermal treatment, suggesting the presence of metastable iron-containing silicates/clays in the sample. The newly formed mineral should be magnetite according to the distinct kink of the cooling curve at ~580 °C.

A partial heating/cooling method [37, 38] was used to investigate magnetic mineralogical changes during thermal
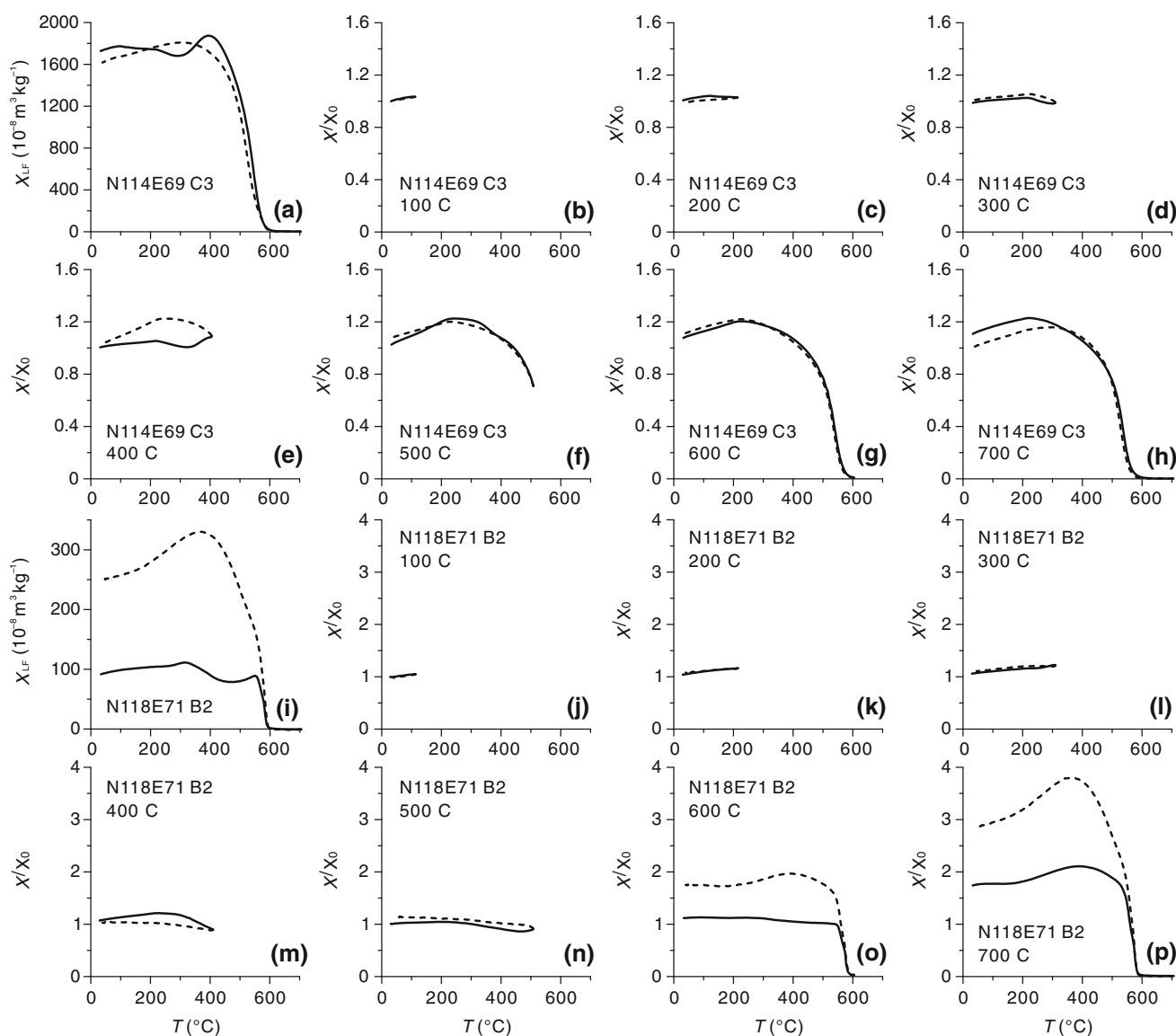
Fig. 4 χ-T curves of representative samples from the burnt area (N114E69 C3) and the unburnt area (N118E71 B2). Note that each sample was separated into two parts: one being continuously exposed through temperature cycle from room temperature to 700 °C and back to the room temperature (**a, i**); and the other, subject to partial heating/cooling runs with the highest temperatures from 100 to 700 °C at an interval of 100 °C (**b–h, j–p**). *Solid* and *dashed lines* show heating and cooling curves, respectively

treatment (Fig. 4b–h, j–p). For the sample from the burnt area (N114E69 C3), except for the 400 °C heating/cooling run, χ-T curves are nearly reversible (Fig. 4b–h). This behavior is well consistent with that of the 700 °C heating/cooling run (Fig. 4a), further indicating that almost no neoformation of ferrimagnetic minerals during thermal treatment. However, for the sample from the unburnt area (N118E71 B2), the heating/cooling runs between 100 and 500 °C are nearly reversible (Fig. 4j–n), while the 600 and 700 °C runs are clearly irreversible (Fig. 4o, p). These results indicate the presence of metastable iron-containing silicates/clays in the sample from the unburnt area, which were transformed to strong magnetic minerals during

thermal treatment. Also, the irreversible heating/cooling runs at 600 and 700 °C illustrate that the sample was not heated up to 600 °C for a certain period of time.

Diffuse reflectance spectrum results are shown in Fig. 5, which indicate that all selected samples contain goethite and hematite. Samples with high redness values (N120E69 B6, N114E69 C3, N118E68 B2, and samples of Localities 2 and 3) contain more hematite. Semiquantitative analysis of the DRS measurements shows that samples of H2 and H3 contain less goethite than hematite, and samples of H1 contain a little bit more goethite than hematite (~ 1.5 times). However, samples from the unburnt areas all contain more goethite than hematite. The goethite content of
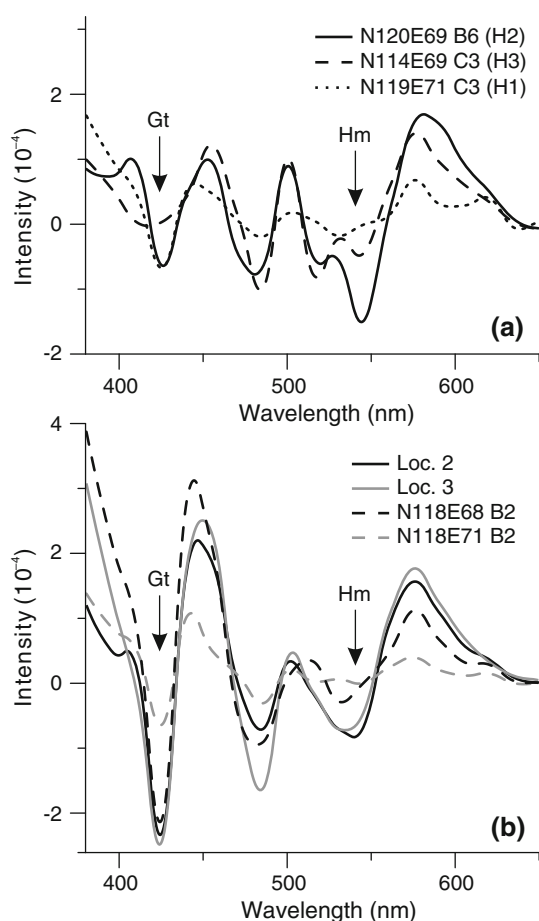
Fig. 5 The second-order derivatives of the K–M functions. Gt and Hm indicate the absorption band of goethite ($\sim$425 nm) and hematite ($\sim$535 nm), respectively [36, 41]

Localities 2 and 3 samples is much higher than that of the excavation area (except for sample N118E68 B2, of which goethite content is close to Localities 2 and 3). The hematite content of Localities 2 and 3 samples is lower than that of the burnt area, but much higher than that of other excavation area.

In summary, samples from both the burnt and unburnt areas contain magnetic minerals of magnetite, hematite, and goethite. However, samples from the burnt areas contain more magnetite and hematite. Difference of magnetic susceptibility and redness in different areas is mainly controlled by the content of magnetite and hematite. High values of magnetic susceptibility and redness in the burnt areas are, respectively, attributable to the newly formed magnetite and hematite grains during heating process.

4 Discussion

Previous researches of field experimental fires show that controlled fires (e.g., campfires, which are usually kept burning over a certain period of time or are burnt repeatedly) generate a significant magnetic enhancement [25]. The post-burn magnetic susceptibility is at least 50 % higher than that of adjacent unburnt control samples [25], and even could be up to 50 times of the pre-burn magnetic susceptibility [20]. Natural burning processes (e.g., tree stump fires, grass fires, etc.) only make very small changes in the magnetic susceptibility of the sediments [25]. Difference between burning temperature of human use of fires and natural fires causes the distinction of magnetic susceptibilities. The highest temperature on surface of the central area of the hearth can be above 600 °C [20]. And a maximum temperature of 860 °C was recorded in the work of Berna et al. [42]. Temperatures of the periphery are much lower, usually below 300 °C [20, 21]. However, natural fires can't generate sufficient heat to produce distinct changes in magnetic mineral of the sediments because of the lower temperatures (usually below 300 °C) [25]. The Peking Man cave at Zhoukoudian was formed in carbonate rock area, where the magnetic susceptibility of bedrock is close to zero. The magnetic susceptibility of the burnt sediments is much higher than that of the bedrock, topsoils in the vicinity of Locality 1 and natural sediments of Localities 2 and 3. Therefore, sediments with extremely high χ_{LF} very likely had experienced high-temperature events. The results of χ-T curves illustrate that sediments of the burnt areas could have been heated up to 700 °C. As mentioned above, temperatures of natural fires are generally much lower. Hence, the distinct enhancement of magnetic susceptibility of the sediments of the burnt area is most likely due to human controlled use of fire.

Transformation of metastable iron-containing silicates/clays to stronger magnetic minerals (e.g., magnetite) leads to the enhancement of magnetic susceptibility [28, 37, 40]. Furthermore, at temperatures between 250 and 400 °C, goethite dehydrates and transforms to hematite [29], which causes the red coloration. Results of DRS show that all samples contain goethite. In samples of H3 and H2, the ratio of goethite to hematite is lower than 1. In sample of H1, even though the ratio is slightly higher than 1, it is still much lower than that of the samples of the unburnt area and Localities 2 and 3. These results indicate that the reduction in the goethite transformed to hematite due to heating. The newly generated hematite caused the reddish color of the rubified sediments in H1 and H2. At Localities 2 and 3, the sediments show reddish hue too, but their χ_{LF} are much lower. The reddish hues should be caused by weathering-generated hematite.

The generation of hematite during heating will not cause the distinct increase of χ_{LF}, since χ_{LF} of hematite is much lower than that of magnetite. Above 400 °C, magnetite can be generated by reduction of hematite [28, 43, 44], which apparently will increases the χ_{LF}. And the results of

SCIENCE CHINA PRESS

χ-T curves illustrate the heating temperature could be above 700 °C.

Heating changes grain size distribution of magnetic particles. Newly generated hematite grains by dehydration of goethite are generally SP [29]. Previous studies show that large amount of ultra-fine (SD and SP) grains are generated during heating [23], and significant amount of SP magnetite grains were detected in burnt clay [30]. χ_{FD} and χ_{FD} % data indicate that the sediments of the burnt area contain large amount of magnetite grains ranging across the SP to SD boundary, which are the major contributor of the high values of χ_{LF}. These grains were very likely to be generated during anthropogenic use of fire.

5 Conclusions

We have examined the burnt and unburnt sediments of the newly excavated area in Layer 4, Locality 1, Zhoukoudian by detailed magnetic, color, and diffuse reflectance spectrum measurements. The main conclusions are:

(1) Sediments from the burnt area have distinctly high values of χ_{LF} and redness, especially those of H3 at south end of the excavation area, whose χ_{LF} is 22 times of the adjacent areas. χ-T curves suggest that these burnt sediments could have been heated above 700 °C.

(2) Burning caused the new formation of large amounts of magnetite and hematite grains, which are responsible for the distinctly high values of χ_{LF} and redness in the burnt area of Layer 4.

(3) Those changes in χ_{LF} and redness are impossibly resulted from natural fires, thus most likely signaling the human activities of controlled use of fire. However, additional work is needed to confirm whether or not these heat-affected sediments were occurred in situ.

References

1. Zhao SS, Pei JX, Guo SL et al (1985) Study of chronology of Peking Man Site. In: Wu RK, Ren ME, Zhu XM et al (eds) Multi-disciplinary study of the Peking Man Site at Zhoukoudian. Science Press, Beijing, pp 239–240 (in Chinese)
2. Shen G, Gao X, Gao B et al (2009) Age of Zhoukoudian *Homo erectus* determined with ^{26}Al/^{10}Be burial dating. Nature 458:198–200
3. Weiner S (2010) Microarchaeology: beyond the visible archaeological record. Cambridge University Press, New York
4. Berna F, Goldberg P, Horwitz LK et al (2012) Microstratigraphic evidence of in situ fire in the Acheulean strata of Wonderwerk Cave, Northern Cape province, South Africa. Proc Natl Acad Sci USA 109:E1215–E1220
5. Black D (1932) Evidences of the use of fire by *Sinanthropus*. Bull Geol Soc Chin 11:107–108
6. James SR (1989) Hominid use of fire in the Lower and Middle Pleistocene: a review of the evidence. Curr Anthropol 30:1–26
7. Renfrew C, Bahn P (1991) Archaeology: theories, methods and practice. Thames and Hudson, London
8. Jia LP, Huang WW (1984) Excavation at Zhoukoudian. Tianjin Science and Technology Press, Tianjin (in Chinese)
9. Guo S, Zhou S, Meng W et al (1980) Fission track dating of Peking Man. Chin Sci Bull 25:700 (in Chinese)
10. Guo S, Liu S, Sun S et al (1991) Fission track dating of the 4th Layer of the Peking Man Site. Acta Anthrop Sinica 10:73–77 (in Chinese)
11. Liu SS, Zhang F, Hu RY et al (1985) Dating Peking Man Site by fission track method. In: Wu RK, Ren ME, Zhu XM et al (eds) Multi-disciplinary study of the Peking Man Site at Zhoukoudian. Science Press, Beijing, pp 241–245 (in Chinese)
12. Qian F, Zhang JX, Yin WD (1985) Magnetic stratigraphy from the sediment of West Wall and Test Pit of Locality 1 at Zhoukoudian. In: Wu RK, Ren ME, Zhu XM et al (eds) Multi-disciplinary study of the Peking Man Site at Zhoukoudian. Science Press, Beijing, pp 251–255 (in Chinese)
13. Grün R, Huang PH, Wu X et al (1997) ESR analysis of teeth from the paleoanthropological site of Zhoukoudian, China. J Hum Evol 32:83–91
14. Weiner S, Xu Q, Goldberg P et al (1998) Evidence for the use of fire at Zhoukoudian, China. Science 281:251–253
15. Goldberg P, Weiner S, Bar-Yosef O et al (2001) Site formation processes at Zhoukoudian, China. J Hum Evol 41:483–530
16. Wu X (1999) Investigating the possible use of fire at Zhoukoudian, China. Science 283:299a
17. Xu Q, Liu J (1998) Comments on "Evidence for the use of fire at Zhoukoudian, China" by Weiner et al. Acta Anthropol Sin 17:318–329 (in Chinese)
18. Le Borgne E (1955) Susceptibilité magnétique anormale du sol superficiel. Ann Géophys 11:399–419
19. Le Borgne E (1960) Influence du feu sur les propriétés magnétiques du sol et sur celles du schiste et du granite. Ann Géophys 16:159–195
20. Carrancho Á, Villalaín JJ (2011) Different mechanisms of magnetisation recorded in experimental fires: archaeomagnetic implications. Earth Planet Sci Lett 312:176–187
21. Linford NT, Canti MG (2001) Geophysical evidence for fires in antiquity: preliminary results from an experimental study. Archaeol Prospect 8:211–225
22. Church MJ, Peters C, Batt CM (2007) Sourcing fire ash on archaeological sites in the Western and Northern Isles of Scotland, using mineral magnetism. Geoarchaeology 22:747–774
23. Herries AIR, Kovacheva M, Kostadinova M et al (2007) Archaeo-directional and -intensity data from burnt structures at the Thracian site of Halka Bunar (Bulgaria): the effect of magnetic mineralogy, temperature and atmosphere of heating in antiquity. Phys Earth Planet Inter 162:199–216
24. Brown KS, Marean CW, Herries AIR et al (2009) Fire as an engineering tool of early modern humans. Science 325:859–862

25. Bellomo RV (1993) A Methodological approach for identifying archaeological evidence of fire resulting from human activities. J Archaeol Sci 20:525–553

26. Morinaga H, Inokuchi H, Yamashita H et al (1999) Magnetic detection of heated soils at Paleolithic sites in Japan. Geoarchaeology 14:377–399

27. Maki D, Homburg JA, Brosowske SD (2006) Thermally activated mineralogical transformations in archaeological hearths: inversion from maghemite γFe_2O_3 phase to haematite αFe_2O_3 form. Archaeol Prospect 13:207–227

28. Carrancho Á, Villalaín JJ, Angelucci DE et al (2009) Rock-magnetic analyses as a tool to investigate archaeological fired sediments: a case study of Mirador cave (Sierra de Atapuerca, Spain). Geophys J Int 179:79–96

29. Dunlop DJ, Özdemir Ö (1997) Rock magnetism: fundamentals and frontiers. Cambridge University Press, Cambridge

30. Jordanova N, Petrovsky E, Kovacheva M et al (2001) Factors determining magnetic enhancement of burnt clay from archaeological sites. J Archaeol Sci 28:1137–1148

31. Stone R (2009) Still seeking Peking Man. Science 325(5936):22–23

32. Jia LP (1959) Report on the excavation of *Sinanthropus* site in 1958. Paleovertebr et Paleoanthropol 1:21–26 (in Chinese)

33. Goldberg P, Macphail RI (2006) Practical and theoretical geoarchaeology. Blackwell Publishing, Malden

34. Teilhard de Chardin P, Young CC (1929) Preliminary report on the Choukoutien fossiliferous deposit. Bull Geol Soc Chin 8:173–202

35. Zhang SS, Song TB (eds) (2003) Beijing annals. World cultural heritage volume. The Peking Man ruins annals. Beijing Publishing House, Beijing (in Chinese)

36. Torrent J, Barrón V (2002) Diffuse reflectance spectroscopy of iron oxides. In: Hubbard AT (ed) Encyclopedia of surface and colloid science. Marcel Dekker, New York, pp 1438–1446

37. Deng C, Zhu R, Jackson MJ et al (2001) Variability of the temperature-dependent susceptibility of the Holocene eolian deposits in the Chinese Loess Plateau: a pedogenesis indicator. Phys Chem Earth Part A 26:873–878

38. Zhu R, Deng C, Jackson MJ (2001) A magnetic investigation along a NW-SE transect of the Chinese Loess Plateau and its implications. Phys Chem Earth Part A 26:867–872

39. Thompson R, Oldfield F (1986) Environmental magnetism. Allen & Unwin, London

40. Deng C, Zhu R, Verosub KL et al (2004) Mineral magnetic properties of loess/paleosol couplets of the central Loess Plateau of China over the last 1.2 Myr. J Geophys Res 109:B01103

41. Torrent J, Barrón V (2003) The visible diffuse reflectance spectrum in relation to the color and crystal properties of hematite. Clays Clay Miner 51:309–317

42. Berna F, Behar A, Shahack-Gross R et al (2007) Sediments exposed to high temperatures: reconstructing pyrotechnological processes in Late Bronze and Iron Age Strata at Tel Dor (Israel). J Archaeol Sci 34:358–373

43. Fine P, Singer MJ, La Ven R et al (1989) Role of pedogenesis in distribution of magnetic susceptibility in two California chronosequences. Geoderma 44:287–306

44. Marmet E, Bina M, Fedoroff N et al (1999) Relationships between human activity and the magnetic properties of soils: a case study in the Medieval site of Roissy-en-France. Archaeol Prospect 6:161–170